AGU ADVANCING EARTH AND SPACE SCIENCE

Earth and Space Science

RESEARCH ARTICLE
10.1029/2020EA001220

# Modeling the Impact of Marine DMS Emissions on Summertime Air Quality Over the Coastal East China Seas

**Shanshan Li[1], Golam Sarwar[2], Junri Zhao[1], Yan Zhang[1,3,4], Shengqian Zhou[1], Ying Chen[1], Guipeng Yang[5], and Alfonso Saiz-Lopez[6]**

[1]Shanghai Key Laboratory of Atmospheric Particle Pollution and Prevention (LAP3), Department of Environmental Science and Engineering, Fudan University, Shanghai, China, [2]Center for Environmental Measurement and Modeling, Office of Research and Development, U.S. Environmental Protection Agency, Research Triangle Park, NC, USA, [3]Shanghai Institute of Eco-Chongming, Shanghai, China, [4]Institute of Atmospheric Sciences, Fudan University, Shanghai, China, [5]Key Laboratory of Marine Chemistry Theory and Technology, Ministry of Education, College of Chemistry and Chemical Engineering, Ocean University of China, Qingdao, China, [6]Department of Atmospheric Chemistry and Climate, Institute of Physical Chemistry Rocasolano, CSIC, Madrid, Spain

**Key Points:**
- The use of local database better reproduces DMS emission fluxes over China's seawater
- The LM86 parameterization (Liss & Merlivat, 1986, https://doi.org/10.1007/978-94-009-4738-2_5) produces the best performance among the three tested schemes in China's offshore waters
- The marine DMS emissions increase $SO_2$ and $SO^4_2$- in the atmosphere of the eastern China Sea

**Supporting Information:**
- Supporting Information S1
- Table S1

**Correspondence to:**
Y. Zhang,
yan_zhang@fudan.edu.cn

**Citation:**
Li, S., Sarwar, G., Zhao, J., Zhang, Y., Zhou, S., Chen, Y., et al. (2020). Modeling the impact of marine DMS emissions on summertime air quality over the coastal East China seas. *Earth and Space Science*, *7*, e2020EA001220. https://doi.org/10.1029/2020EA001220

Received 10 APR 2020
Accepted 18 SEP 2020
Accepted article online 25 SEP 2020



**Abstract** Biogenic emission of dimethyl sulfide (DMS) from seawater is the major natural source of sulfur into the atmosphere. In this study, we use an advanced air quality model (CMAQv5.2) with DMS chemistry to examine the impact of DMS emissions from seawater on summertime air quality over China. A national scale database of DMS concentration in seawater is established based on a 5-year observational record in the East China seas including the Bohai Sea, the Yellow Sea, and the East China Sea. We employ a commonly used global database and also the newly developed local database of oceanic DMS concentration, calculate DMS emissions using three different parameterization schemes, and perform five different model simulations for July, 2018. Results indicate that in large coastal areas of China, the average DMS emissions flux obtained with the local database is 3 times higher than that resulting from the global database, with a mean value of 9.1 μmol $m^{-2}$ $day^{-1}$ in the Bohai Sea, 8.4 μmol $m^{-2}$ $day^{-1}$ in the Yellow Sea, and 13.4 μmol $m^{-2}$ $day^{-1}$ in the East China Sea. The total DMS emissions flux calculated with the Nightingale scheme is 42% higher than that obtained with the Liss and Merlivat scheme but is 15% lower than that obtained with the Wanninkhof scheme. Among the three parameterizations, results of the Liss and Merlivat scheme agree better with the ship-based observations over China's coastal waters. DMS emissions with the Liss and Merlivat parametrization increase atmospheric sulfur dioxide ($SO_2$) and sulfate ($SO_4^{2-}$) concentration over the East China seas by 6.4% and 3.3%, respectively. Our results indicate that although the anthropogenic source is still the dominant contributor of atmospheric sulfur burden in China, biogenic DMS emissions source is nonnegligible.

## 1. Introduction

Oceanic dimethylsulfide (DMS:$CH_3SCH_3$) emission is the dominant natural source of atmospheric sulfur (Andreae & Raemdonck, 1983; Bates et al., 1992). Once released to the atmosphere, DMS is oxidized to sulfur dioxide ($SO_2$) and methane sulfonic acid (MSA), which can subsequently be further oxidized to sulfuric acid or sulfate ($SO_4^{2-}$). MSA is an important natural component of acid rain, and marine biogenic $SO_4^{2-}$ is the main component of atmospheric particulate matter that can participate in cloud formation, affecting atmospheric radiation balance and climate (Charlson et al., 1987).

Despite the substantial progress made during the last 30–40 years, the specific DMS oxidation pathways are still not very well understood (Barnes et al., 2006; Hoffmann et al., 2016; Ravishankara et al., 1997). The reaction of hydroxyl radical (OH) with DMS is perhaps the most studied of all reactions involving DMS and is one of the most complex reactions as OH radical both adds to and abstracts from DMS. Contrary to abstraction, the rate of the addition reaction increases with decreasing temperature (Atkinson et al., 2004; Zhu et al., 2006). The reaction of DMS with nitrate radical ($NO_3$) is important at night and in the polluted atmosphere (Stark et al., 2007). Nevertheless, halogens contribute significantly to DMS oxidation, which are ignored in many air quality models. Noteworthy is the reaction of DMS with bromine oxide (BrO), which could be particularly important as a sink for DMS especially when BrO mixing

ratios can reach 0.5 parts per trillion by volume (pptv), accounting for approximately 16% of DMS removal in the atmosphere (Breider et al., 2010; Toumi, 1994). Analogous to BrO oxidation, the reaction of other halogen oxides with DMS could also be potentially significant in the regions of the remote marine boundary layer (Hoffmann et al., 2016; von Glasow & Crutzen, 2004; von Glasow et al., 2002). In marine regions affected by continental pollution, the reactions of molecular iodine ($I_2$) and hypoiodous acid (HOI) with $NO_3$ can also indirectly affect DMS, increasing its levels about 20% at night (Saiz-Lopez et al., 2016). Indeed, very high spatial resolution (4 km) simulations have shown how the coupling of DMS and halogen ocean emissions can significantly affect the air quality of a coastal megacity such as Los Angeles (United States) (Muñiz-Unamunzaga et al., 2018). The levels of ozone, $NO_3$, and $HO_x$ were decreased, but the average concentration of secondary organic aerosol increased, which was due to the increase in aerosol acidity and sulfate aerosol formation when DMS and bromine are combined. Therefore, the DMS chemistry in the model should at least include the DMS oxidation by hydroxyl, nitrate, and halogen oxides for more accurate simulation results.

Bates et al. (1992) reported that DMS emission flux accounted for 90% of total marine sulfur emissions. Many researchers have subsequently used different methods to estimate the global sea-to-air flux of DMS. For example, Putaud and Nguyen (1996) reported global estimates of 17–21 Tg S $a^{-1}$, Lana et al. (2011) reported estimates of 17.6–34.4 Tg S $a^{-1}$, and Andreae and Raemdonck (1983) reported an estimate of 38.5 Tg S $a^{-1}$. The sea-to-air flux of DMS is dependent on the DMS concentration in seawaters and the sea-to-air transfer velocity, which varies with sea surface temperature (SST) and wind speed (Liss & Merlivat, 1986; Nightingale et al., 2000; Wanninkhof, 1992). There have been multiple efforts to accurately represent the global climatological sea surface DMS concentration distribution. The major effort, initiated by Kettle et al. (1999), was to compile a now freely available database using DMS measurements contributed by individual scientists. They used 15,617 surface DMS observation data from 134 voyages and interpolated them into the global ocean with 3,317 grids at a resolution of 1° × 1° to represent the global DMS concentration distribution. Lana et al. (2011) expanded the database to over 47,000 DMS measurements covering the measured data from 1972 to 2010, among which about 64% of the data were collected in the Northern Hemisphere and 36% in the Southern Hemisphere, generating them into monthly climatological fields of sea surface DMS concentration (freely available at http://tinyurl.com/yc7moge). The effects of this DMS climatology on global cloud microphysics and aerosol have been previously studied (Mahajan et al., 2015). The Global Surface Seawater DMS Database (http://saga.pmel.noaa.gov/dms/) continues to be updated by the DMS community. However, the number of observations available in the database is still fairly small, especially over China waters. The establishment of a local DMS concentration database that is more suitable for regional simulation in China is necessary.

China's marine scientists has been studying the distribution of DMS in China's seas since 1993. Hu et a1. (2003) first established the analysis method of DMS and conducted a preliminary study on DMS concentration and sea-to-air flux on the eastern coast of China. Many researchers subsequently conducted considerable on-site observations and studied the horizontal and vertical distribution of DMS and its correlations with the bioenvironmental factors in certain areas of the Bohai Sea, the Yellow Sea, the East China Sea, and the South China Sea (Li et al., 2016; Yang et al., 1999, 2012; Yang, Zhang, et al., 2015; Zhang et al., 2017), providing great data support for subsequent modeling research activities. While research on DMS in China seawater is comparatively mature, there has been little systematic research on atmospheric DMS and its chemical behavior over the continental shelf of eastern China. Xu et al. (2016) simulated the global DMS sea-to-air flux with the Community Earth System Model and found significant DMS emission flux in the highly productive eastern China seas. However, higher spatial resolution simulations are necessary to better quantify the flux of DMS from the oceans in China to investigate its impact on air quality in China's coastal area.

The main objective of this study is to examine the impacts of DMS emissions on $SO_2$ and $SO_4^{2-}$ in the atmosphere over China during summer. A database of DMS concentrations in seawater in China is established for estimating DMS fluxes in China. Moreover, by comparing the results of different parameterization schemes for DMS emission fluxes, we determine the most suitable parametric method for Chinese seas. This paper is a starting point to further explore the long-term environmental impacts of DMS emissions in China.

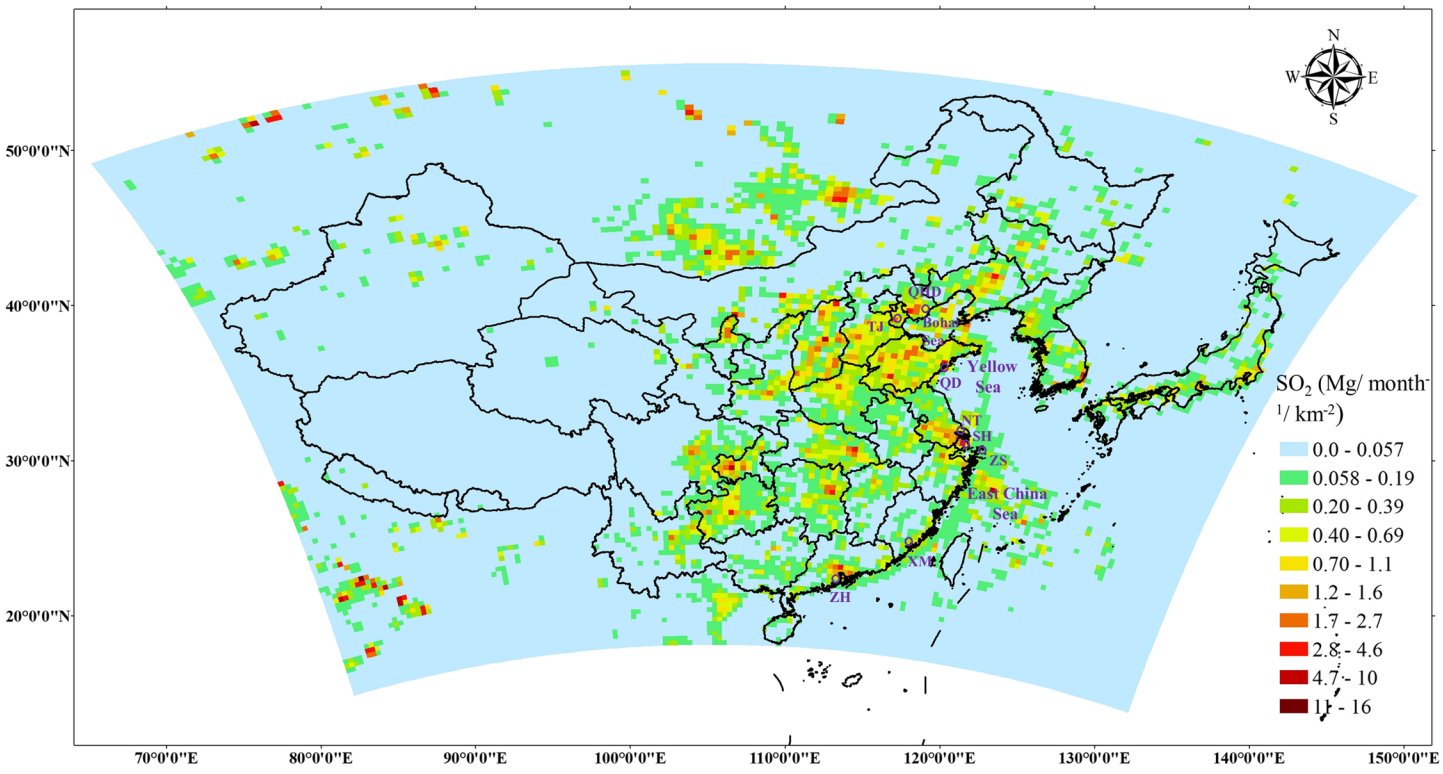


**Figure 1.** The spatial distribution of $SO_2$ emission from anthropogenic emissions for July 2018. The colored geographic area was the model domain covering the Bohai Sea, the Yellow Sea, and the East China Sea. Eight coastal cities are marked with purple circles (ZH: Zhuhai, XM: Xiamen, ZS: Zhoushan, SH: Shanghai, NT: Nantong, QD: Qingdao, TJ: Tianjin, and QHD: Qinghuangdao). $SO_2$ emissions (mg/month/km$^{-2}$) were calculated on a monthly basis for five sectors: Power, industry, residential, transportation in land area, and shipping emission (with the spatial resolution of 36 × 36 km).

## 2. Model Setup

### 2.1. Model Description

The U.S. Environmental Protection Agency's (EPA) Model-3/Community Multiscale Air Quality (CMAQ) model, version 5.2 (www.epa.gov/cmaq; https://doi.org/10.5281/zenodo.1167892) was used in this study with 36 × 36 km horizontal grid spacing and a 27-layer vertical structure for the domain covering the geographic area shown in Figure 1. CMAQv5.2 model does not include any DMS chemistry. Sarwar et al. (2015, 2018, 2019) combined the Carbon Bond chemical mechanism with atmospheric bromine, chlorine, iodine, and DMS chemistry and incorporated it into the hemispheric CMAQ model (Mathur et al., 2017). We used their atmospheric chemistry, which includes gas-phase oxidation of DMS by OH, $NO_3$, chlorine radical (Cl), chlorine monoxide (ClO), iodine monoxide (IO), and BrO. The detailed reactions are provided in Table S1 in the supporting information. The model was configured to use the AERO6 aerosol module.

Considering the highest concentration of DMS in seawater in summer and that the wind typically flows from ocean to land during the summer monsoon, the simulation period covered from 1 to 31 July in 2018 with a 15-day spin-up period. The emission data used in this study is described in detail in section 2.2. The meteorological field required for the CMAQ model was generated by the Weather Research and Forecasting (WRFv3.6) model (Skamarock & Klemp, 2008) and processed by the MCIPv4.3 (Meteorology-Chemistry Interface Processor) (Otte & Pleim, 2010). The meteorological input data was generated from the Chinese National Centers for Environmental Predictions Final Analysis with a spatial resolution of 1° × 1° and a temporal resolution of 6 hr. Monthly mean boundary conditions without and with DMS chemistry were generated from the corresponding hemispheric CMAQ model results (Sarwar et al., 2018) and were used in this study.

### 2.2. Emission Inventories

In this study, the anthropogenic emissions consisted of three parts: (1) Multi-resolution Emission Inventory for China (MEIC) (http://meicmodel.org/dataset-meic.html), (2) MIX inventory: a mosaic

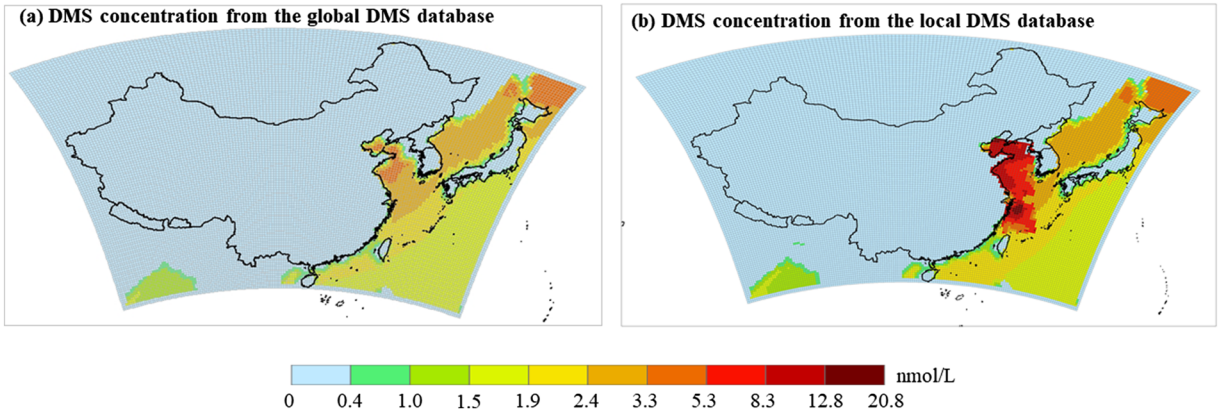


**Figure 2.** DMS concentration in seawater from (a) the Global Surface Seawater DMS Database (http://saga.pmel.noaa.gov/dms/) and (b) the local database for the summer season.

Asian anthropogenic emission inventory under the international collaboration framework of the Model Inter-Comparison Study for Asia and the Task Force on Hemispheric Transport of Air Pollution for areas of other countries (Li et al., 2017), and (3) shipping emissions, which was also relatively important for studying the marine biogenic gases (Fan et al., 2016). Affected by the energy conservation and emission reduction policies, the emissions of pollutants in China in recent years have changed considerably. The MEIC and MIX inventories used the latest available emission data, with the MEIC inventory for the year of 2016 and the MIX inventory for the year of 2010. The shipping emissions were calculated using the model developed by Fan et al. (2016), and the detailed principle and method have been previously described (Feng et al., 2019). The spatial distributions of $SO_2$ emissions generated by human activities are shown in Figure 1. High $SO_2$ emissions persisted in the eastern part of China, and the total anthropogenic $SO_2$ emissions in the entire domain were $1.7 \times 10^6$ tons in July, in which shipping emissions accounted for 59, 000 tons.

### 2.3. Database of Observed DMS Concentrations in Seawater

In previous studies, researchers mainly obtained DMS concentrations from the Global Surface Seawater DMS Database (http://saga.pmel.noaa.gov/dms/) (Lana et al., 2011). However, the global DMS data are rare and relatively old (in 1993–1994) for China's coastal waters, which may be inconsistent with the current conditions and could lead to unrealistic DMS estimates. To represent the contemporary conditions in China's seawater, we use a long-term DMS observation data set for the summer season (June, July, and August) in 2011, 2013, 2015, 2016, and 2017 from a series of cruise survey experiments led by the China Ocean University (Yang, Yang, et al., 2015; Yang, Zhang, et al., 2015) and calculated 5-year mean values where the observation data existed and performed interpolation to map DMS concentrations in Chinese seas. In oceanic areas not covered by the cruise survey, the default values from the global DMS database are still used. Here, the resulting database is termed as the local data set.

The spatial distribution of DMS concentrations from the global DMS database is shown in Figure 2a. The high DMS concentration reaches up to 4 nmol/L in the Bohai Sea and the Yellow Sea. With increasing distance from the shore, the concentration of DMS gradually decreases to less than 2 nmol/L. The spatial distribution of DMS concentrations from the local database is shown in Figure 2b. The use of local DMS observation enhances DMS concentrations in seawater in China. The concentrations of DMS in the local database are 10–20 nmol/L higher than those in the global database in the Bohai Sea and the East China Sea. The DMS concentrations in the local database are in good agreement with the DMS observations of 5.9–27.6 nmol/L in the Bohai Sea (Yang et al., 2014) and 1.8–12.2 nmol/L in the East China Sea (Yang et al., 2011) during June and July. Thus, the use of DMS concentrations from the global database significantly underestimates DMS concentration in China's seawaters, which underscores the need for a local DMS database. Local databases in different seasons also show consistent patterns (Li et al., 2020).

### 2.4. Parameterizations of Air-Sea Gas Exchange

The ocean-atmosphere flux of DMS ($F_{DMS}$) is computed as the product of the concentration gradient between air and water ($\Delta c$) and the total resistance to gas-transfer ($k_T$) at the air/sea interface (Equation 1) (Lana et al., 2011):

$$F_{DMS} = k_T \cdot \Delta c = k_T \cdot \left(C_w - C_g H\right) \approx k_T \cdot C_w \tag{1}$$

where $C_w$ is DMS concentration in seawater, $C_g$ is DMS concentration in air, $H$ is Henry's law coefficient. In general, the concentration of DMS in seawater is approximately 3 orders of magnitude higher than the concentration of DMS in air, so the $C_g/H$ term can just be neglected.

The total gas transfer velocity $k_T$ can be further obtained by air-side ($k_a$) and water-side ($k_w$) transfer velocities when the air resistance cannot be ignored especially at low temperatures and high wind speeds, of which $\gamma_a$ is the atmospheric gradient fraction, a measure of the fraction contribution of total concentration difference driving air-water gas transfer in the air (Equations 2 and 3) (Lana et al., 2011; McGillis et al., 2000):

$$k_T = k_w \cdot (1 - \gamma_a) \tag{2}$$

$$\gamma_a = 1/\left(1 + \frac{k_a}{H k_w}\right) \tag{3}$$

The air-side transfer velocity $k_a$ is calculated based on Kondo (1975) (Equation 4)

$$k_a = 659 \cdot U_{10}/\sqrt{(M_{DMS}/M_{H_2O})} \tag{4}$$

where $U_{10}$ is 10-m wind speed and $M_{DMS}$ and $M_{H2O}$ are the molecular weights of DMS and water, respectively.

It is the water-side transfer velocity $k_w$ that is often needed to be parameterized in relation to wind speed with different dependencies. In this study, three empirical gas exchange parameterizations are used to quantify the wind speed dependence of the coefficient $k_w$ (Liss & Merlivat, 1986 (LM86); Nightingale et al., 2000 (N00); Wanninkhof, 1992 (W92)). The LM86 parameterization, originally developed for carbon dioxide ($CO_2$), is a piecewise linear function for three wind regimes: the smooth surface regime ($U_{10} \leq 3.6$ m/s), rough surface regime ($3.6 < U_{10} \leq 13$ m/s), and breaking wave regime ($U_{10} > 13$ m/s). The $k_w$ has its calculation formula for each of these regimes:

$$k_w = \begin{cases} 0.17 \times U_{10}/(Sc_{DMS}/600)^{2/3} & U_{10} \leq 3.6\ m/s \\ (2.85 \times U_{10} - 9.65)/(Sc_{DMS}/600)^{1/2} & 3.6 < U_{10} \leq 13\ m/s \\ (5.9 \times U_{10} - 49.3)/(Sc_{DMS}/600)^{1/2} & U_{10} > 13\ m/s \end{cases} \tag{5}$$

where the value 600 is the Schmidt number for $CO_2$ at 20°C. The Schmidt number of DMS ($S_{C_{DMS}}$) is the ratio of the diffusion coefficient of DMS to the absolute viscosity of seawater. According to Saltzman et al. (1993), it can be constructed as a function of SST ($T$/°C) (Equation 6):

$$Sc_{DMS} = 2674.0 - 147.12 \times T + 3.726 \times T^2 - 0.038 \times T^3 \tag{6}$$

The W92 parameterization is more suitable for $k_w$ estimates with short-term or instantaneous wind speed and uses the quadratic equation of wind speed (Equation 7). Considering aspects of both the LM86 and W92 parameterizations, the N00 parameterization was also proposed intermediate between these two schemes (Equation 8):

$$K_w = 0.31 \times {U_{10}}^2/\sqrt{(Sc_{DMS}/600)} \tag{7}$$

$$K_w = \left(0.222 \times {U_{10}}^2 + 0.33 \times U_{10}\right)/\sqrt{(Sc_{DMS}/600)} \tag{8}$$

**Table 1**
*Description of Simulations Performed in This Study*

| Cases | With DMS chemistry | Oceanic DMS concentration data | Parameterization of DMS emission |
|---|---|---|---|
| Case A | No | — | — |
| Case B | Yes | Default global data set | Liss & Merlivat (1986) (LM86) |
| Case C | Yes | Localized data set | Liss & Merlivat (1986) (LM86) |
| Case D | Yes | Localized data set | Nightingale et al. (2000) (N00) |
| Case E | Yes | Localized data set | Wanninkhof (1992) (W92) |

Model calculates DMS emissions using the monthly average DMS concentration and temporally resolved meteorological parameters at each model time step, and these emissions are released into the first vertical layer of the model.

### 2.5. Simulation Cases

Five simulations were performed as shown in the Table 1. One simulation (Case A) did not include any DMS emissions. Four additional simulations (Cases B–E) were performed to examine the impacts of DMS emissions on model results. DMS emissions in Case B were calculated using the LM86 parameterization and the DMS concentration in seawater from the global DMS data set. In Case C, DMS emissions were calculated using the LM86 parameterization and the DMS concentrations in seawater from our local DMS database. Case D employed the N00 parameterization and the DMS concentrations in seawater from the local DMS database, while Case E employed the W92 parameterization and also the local DMS database. The same atmospheric chemistry (Sarwar et al., 2018) was used in all cases. We analyzed the model results to determine the best scheme suitable for simulating the impact of DMS emissions on air quality over Chinese seawater.

## 3. Results

### 3.1. Simulated Distributions of Atmospheric DMS Concentration and Emission Flux

As described in section 2.5, the LM86 (Liss & Merlivat, 1986) parameterization was used in Case B and Case C to calculate the DMS emission flux utilizing the 10-m wind speed and the SST from the WRF model. By comparing the results of the two cases, the performance of the local database compared to the global database can be examined.

#### 3.1.1. Simulation Based on Global Scale DMS Database

Calculated DMS emission flux for Case B generally ranges between 1 and 5 μmol $m^{-2}$ $day^{-1}$, with a maximum of 6.2 μmol $m^{-2}$ $day^{-1}$ (Figure 3a). The emissions of DMS from the four seas of China and some portion of the Philippine Sea, where the South China Sea extends to, are higher than those of the Sea of Japan. Such higher values may correlate with the high productivity due to the high riverine loads of nutrients and organic materials in the shelf area in summer. The results of this simulation, however, are overwhelmingly lower than the estimates of 0.2–36.4 μmol $m^{-2}$ $day^{-1}$ in the North Yellow Sea (Yang et al., 2009), 0.6–34.0 μmol $m^{-2}$ $day^{-1}$ in the East China Sea (Li et al., 2015), and 0.2–15.1 μmol $m^{-2}$ $day^{-1}$ in the northern portion of the South China Sea (Shen et al., 2016) calculated using the observed surface seawater DMS concentrations.

The concentration of DMS in the atmosphere is presented in Figure 3b. Compared to the concentration in seawater, the DMS concentration in the atmosphere is about 3 orders of magnitude lower, which supports the simplifying assumption made for calculating DMS emissions flux in air quality models. The surface layer atmospheric DMS concentration ranges between 20 and 60 pptv with a mean value of about 55 pptv over China's coastal waters. Similar to the distribution of DMS concentration in seawater, the distribution of atmospheric DMS concentration in the Bohai Sea, the Yellow Sea, and the East China Sea is slightly higher than that in the surrounding waters.

#### 3.1.2. Simulation Based on the Local DMS Database

Figures 3c and 3d show the distribution of the monthly mean DMS emission flux and concentration in the atmosphere for Case C. The use of local DMS database results in higher emission fluxes over the Bohai Sea, the East China Sea, and other offshore sea areas, which, in turn, increases DMS atmospheric concentrations over these areas. As shown in the Figure 3c, the distribution of the DMS emission flux is closely related to the DMS sea surface distribution. The DMS emission fluxes vary considerably from $2.9 \times 10^{-8}$ μmol $m^{-2}$ $day^{-1}$

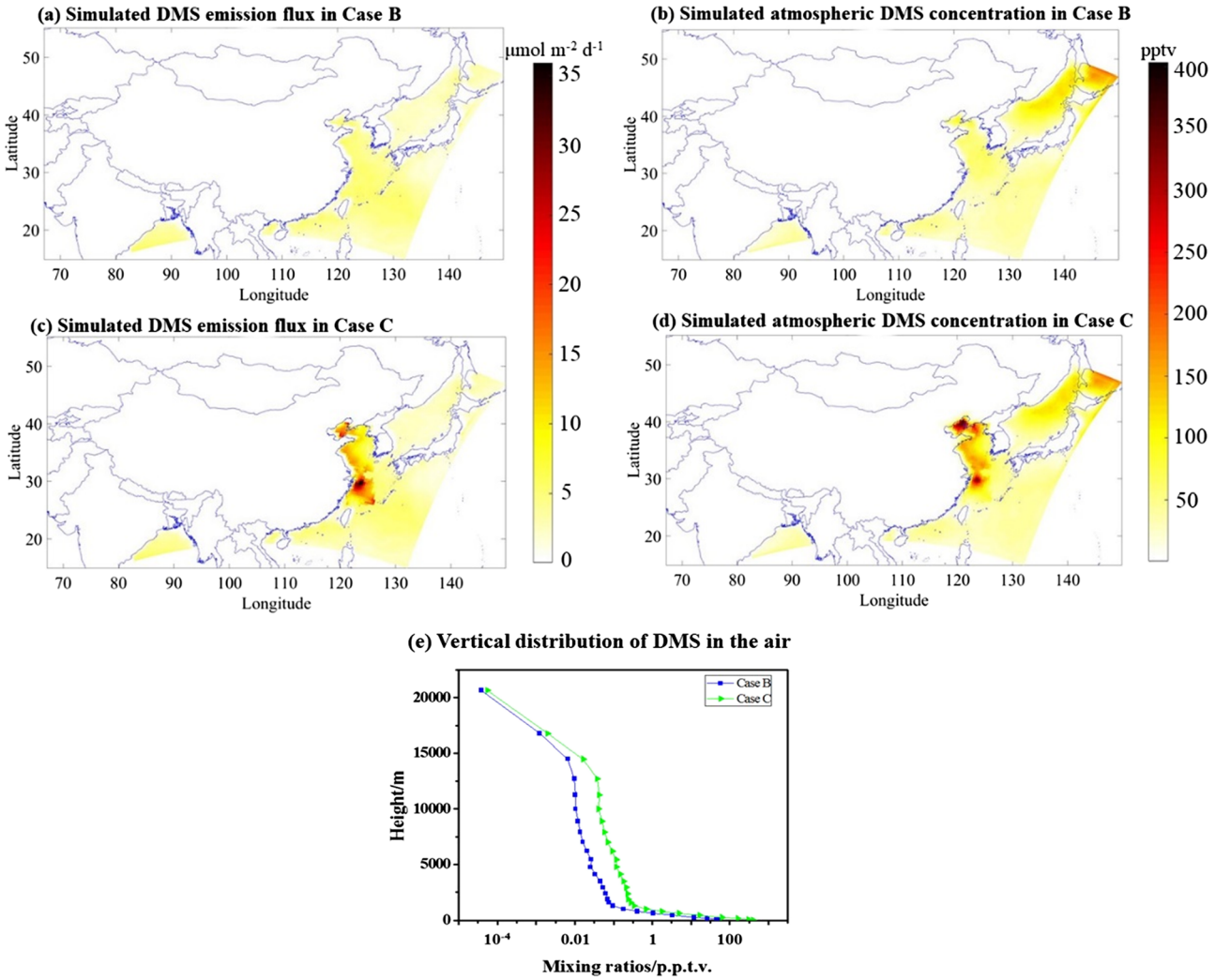


**Figure 3.** The distribution of simulated monthly mean DMS emission fluxes based on a the global DMS database (Case B) and (b) the localized DMS database (Case C) and the (c, d) monthly mean horizontal distribution of atmospheric DMS concentration for Cases B and C and (e) vertical distribution of atmospheric DMS concentration at a grid cell over the Bohai Sea for the two cases.

in the Bay of Bengal to 35.9 μmol $m^{-2}$ $day^{-1}$ in the East China Sea. In contrast with the global database, the local DMS database produces higher fluxes in the shelf area, which is consistent with previous studies (Li et al., 2015; Yang et al., 2009). In order to facilitate the comparison between the two cases, the DMS flux estimates for the Bohai Sea, the East China Sea, and the Yellow Sea in the two cases are summarized in Table 2. In the early work, DMS fluxes were estimated to be 5.56 μmol $m^{-2}$ $day^{-1}$ in summer in the continental shelf zone of the East China Sea (Uzuka et al., 1996). Recently, DMS fluxes were measured on average 6.87 μmol $m^{-2}$ $day^{-1}$ in the North Yellow Sea and 7.45 μmol $m^{-2}$ $day^{-1}$ in the East China Sea and Yellow Sea in summer (Yang et al., 2009, 2011). Clearly, modeled sea-to-air fluxes of DMS in coastal waters is in good agreement with the high flux values that were previously reported. However, compared with observation, the CMAQ model can better reproduce the spatial distribution of DMS fluxes over the entire region and lay the foundation for future research on the impact on climate effects. Besides, the average DMS emission flux in Case C is 30% higher than that in Case B in the entire simulated sea area and is a factor of 3 higher in the area covered by the local DMS database than the global data set, illustrating the profound impact of the local DMS concentration database on DMS flux estimates.

**Table 2**
*Estimated Monthly DMS Emission Flux in Different Sea Areas (Unit: μmol $m^{-2}$ $day^{-1}$)*

| Cases | Bohai Sea | Yellow Sea | East China Sea | Total Sea areas |
|---|---|---|---|---|
| Default global data set | 2.1 | 3.2 | 4.5 | 2.9 |
| Localized data set | 9.1 | 8.4 | 13.4 | 3.7 |

High DMS atmospheric concentrations are predicted over the coastal and shelf areas in the Bohai Sea and the East China Sea (Figure 3d), which generally agree with the simulated high DMS flux in this region. This suggests that variations in DMS concentrations in seawater are largely responsible for the variations in atmospheric DMS levels during the simulation period. However, the spatial pattern of atmospheric DMS concentration does not exactly follow that of the flux distribution. For example, the Bohai Sea has a smaller area of high flux, but a larger area of high atmospheric DMS concentration, and the East China Sea has exactly the opposite pattern. This is the result of atmospheric DMS concentration being also affected by turbulent vertical exchange in the marine boundary layer and by the chemical conversion of DMS to other sulfur species. Figure 3e shows the vertical DMS profile at a grid with the highest surface-layer atmospheric concentration (403 pptv) in Case C over the Bohai Sea. The atmospheric DMS concentration decreases exponentially with altitude and becomes negligible at 800–1,000 m. However, we cannot verify the model predictions since no high-altitude measurements over China's seawater are currently available. The order of magnitudes in this model study are similar to those observed by Jenny et al. (2010) in the high Arctic in summer. This emphasizes the need for aircraft-based measurements over China's waters.

A 2018 Cruise Survey Experiment was conducted in the East China seas during 27 June to 20 July 2018 by the Ocean University of China, in which more than 20 atmospheric DMS samples were collected and analyzed. At each sampling location during the cruise, a clean and evacuated stainless steel Summa® Canister was placed at 10 m above the sea floor facing the windward direction on the front deck for collecting atmospheric samples. Figure S1 shows the spatial pattern of simulated atmospheric surface layer DMS concentrations compared to the atmospheric DMS concentration measured in the 2018 Cruise Survey Experiment. Different concentrations are represented by different colors, of which red points indicate stations with a mixing ratio of more than 210 pptv. The highest concentrations in Case C are simulated at station H2 (219 pptv) and P1 (285 pptv), which are in good agreement with the measured high concentrations at station H2 (213 pptv) and P1 (284 pptv). In contrast, the modeled value is only 96 pptv at H2 and 60 pptv at P1 for Case B. The observations of atmospheric DMS concentration are 32% (on average) higher than the results for Case B but 8.6% lower than that in Case C, again verifying the large impact of local database on simulation results. It should be noted that the local database does not include the DMS concentration in seawater during the simulation period. Compared with the multiyear average of DMS seawater concentrations in this region, the high concentration of DMS in seawater in July 2018 is consistent in the Bohai Sea and the near shore of East China Sea, but without the effects of the averaging and interpolation, the concentration in the Yellow Sea and farther away from the East China Sea is not so high. This produces some larger DMS predictions for Case C compared to the observations. In addition, DMS fluxes are particularly sensitive to wind speeds, and slight changes in the wind speed can affect the DMS flux and the subsequent atmospheric DMS concentration (Tesdal et al., 2016). The simulated wind speed at station C2 (6.8 m/s), D4 (8.0 m/s), and F2 (9.8 m/s) from the WRF model is higher than the observed local wind speed of 1.1, 5, 5.4 m/s, respectively. This also results in higher predicted DMS mixing ratios than observed values.

### 3.2. Impacts of Different Parameterization Schemes

Accurate estimates of sea-to-air flux of DMS are essential to understand the global cycling of biogenic sulfur and its effect on the Earth's radiation budget. Three commonly used parameterizations of LM86 (Liss & Merlivat., 1986), N00 (Nightingale et al., 2000) and W92 (Wanninkhof, 1992) are used to calculate the water-side transfer velocity which can affect DMS flux estimates. We estimate a total DMS flux of 0.068 Tg S $month^{-1}$ using the W92 parameterization, 0.060 Tg S $month^{-1}$ using the N00 parameterization, and 0.044 Tg S $month^{-1}$ using the LM86 parameterization over the modeling domain. The LM86 parameterization uses a linear function of wind speed and consequently produces the lowest estimate of DMS flux. In contrast, the W92 parameterization uses a quadratic function of wind speed and produces the highest estimate of DMS flux. The N00 parameterization uses a combination of linear and quadratic functions and produces an intermediate estimate. Tesdal et al. (2016) adopted the same three parameterizations and reported global estimates of 18–24 Tg S $year^{-1}$; the LM86 parameterization produced the lowest estimate, the N00 produced an intermediate estimate, while the W92 parameterization produced the highest estimate. Lana et al. (2011) reported global DMS fluxes of 17.6, 28.1, and 34.4 Tg S $year^{-1}$ using the LM86, N00, and W92 parameterizations, respectively. Consistent with these previous studies, our calculations also show that the W92 parameterization produces the highest estimate, the N00 parameterization produces an intermediate

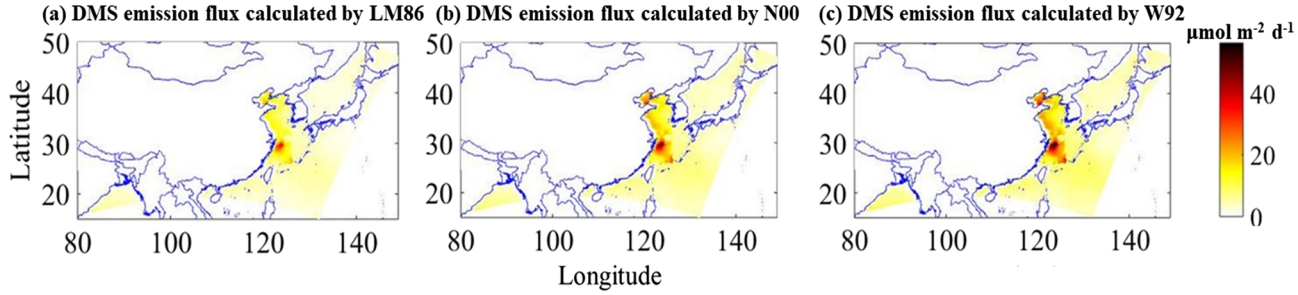


**Figure 4.** The distribution of DMS emission flux obtained with different parameterization schemes: (a) LM86 (Liss & Merlivat, 1986), (b) N00 (Nightingale et al., 2000), and (c) W92 (Wanninkhof, 1992).

estimate, and the LM86 parameterization the lowest estimate of DMS flux. In the Lana et al. (2011) study, the N00 parameterization produced 60% higher estimate than the LM86 parameterization value, while the W92 parameterization produced 22% higher estimate than the N00 parameterization value. In our calculation, the N00 parameterization produces 42% higher flux than the LM86 parameterization value and the W92 parameterization produces 15% higher flux than the N00 parameterization value. Thus, the relative distribution of our estimates of DMS emissions over the Chinese seawater with different parameterizations is somewhat different than the values reported by other investigators for global emission estimates due primarily to the spatiotemporal differences between the studies. All three parameterizations show high fluxes in East China Sea and the Bohai Sea (Figure 4).

Predicted atmospheric DMS concentrations are compared to observed data from the 2018 Cruise Survey Experiment (Figure 5). Simulated atmospheric DMS concentrations corresponding to different sampling times and locations are extracted from the model results and compared with the observations. Observed concentrations range between 10 and 765 ppt. There are few studies on the atmospheric concentration of DMS in China. Ma et al.'s (2004) research on the coastal waters of Qingdao found that the average concentration of DMS in the summer atmosphere was 92.6 pptv. The average concentration of DMS in the atmosphere over the North Yellow Sea in summer was 112.2 pptv (Zhang et al., 2009). Predicted concentrations vary with each parametrization. The W92 parametrization produces the highest concentrations, the LM86 parametrization produces the lowest concentrations, and the N00 parametrization produces intermediate levels of concentrations. We use normalized mean bias and root-mean-square error to calculate the degree of deviation between the observed data and modeling results (Eder & Yu, 2007). The atmospheric concentration of the DMS simulated by the LM86 parameterization is underestimated by 8.6%, while the N00 and W92 schemes overestimate the observed data by 24.7% and 34.5%, respectively. The RMSEs range from 170 pptv (LM86) to 186 pptv (W92). Some studies have suggested that the N00 scheme gives more reasonable results for DMS simulations (Boucher et al., 2003; Marandino et al., 2009). However, we find that the LM86 scheme produces the best performance among the three parameterizations. Such a difference occurs due to the use of the locale database in which DMS concentrations in seawater are higher than those in the global database.

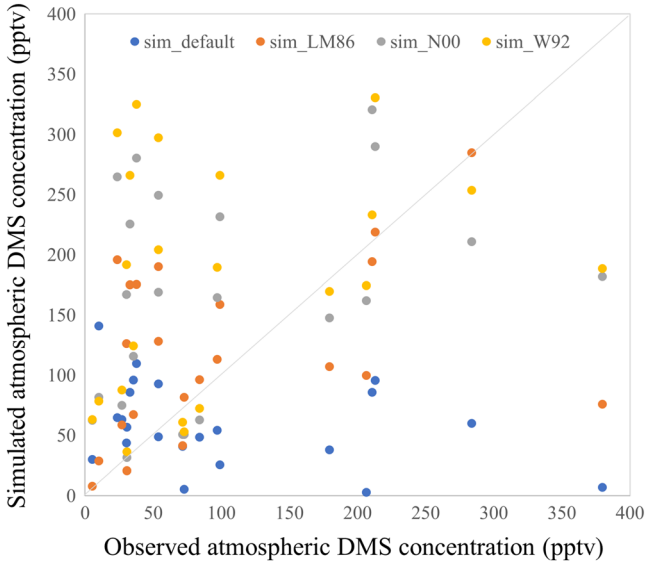


**Figure 5.** A comparison of predicted atmospheric DMS mixing ratios (sim_default: Case B with the global DMS database; sim_LM86, sim_N00, and sim_W92 use the local database and represents Case C with Liss & Merlivat, 1986 parameterization, Case D with Nightingale et al., 2000 parameterization, and Case E with Wanninkhof, 1992 parameterization, respectively) with observed data at different sampling stations. See Figure S1 for locations of the sampling stations.

### 3.3. Impacts of DMS Chemistry on Air Quality

The utilization of the LM86 scheme (Case C) generates the most optimum results (section 3.2). Thus, we use results obtained in Case C and A (without the DMS emissions) to estimate the contribution of marine DMS emissions to atmospheric $SO_2$ and $SO_4^{2-}$ concentrations in the atmosphere over China's seas.

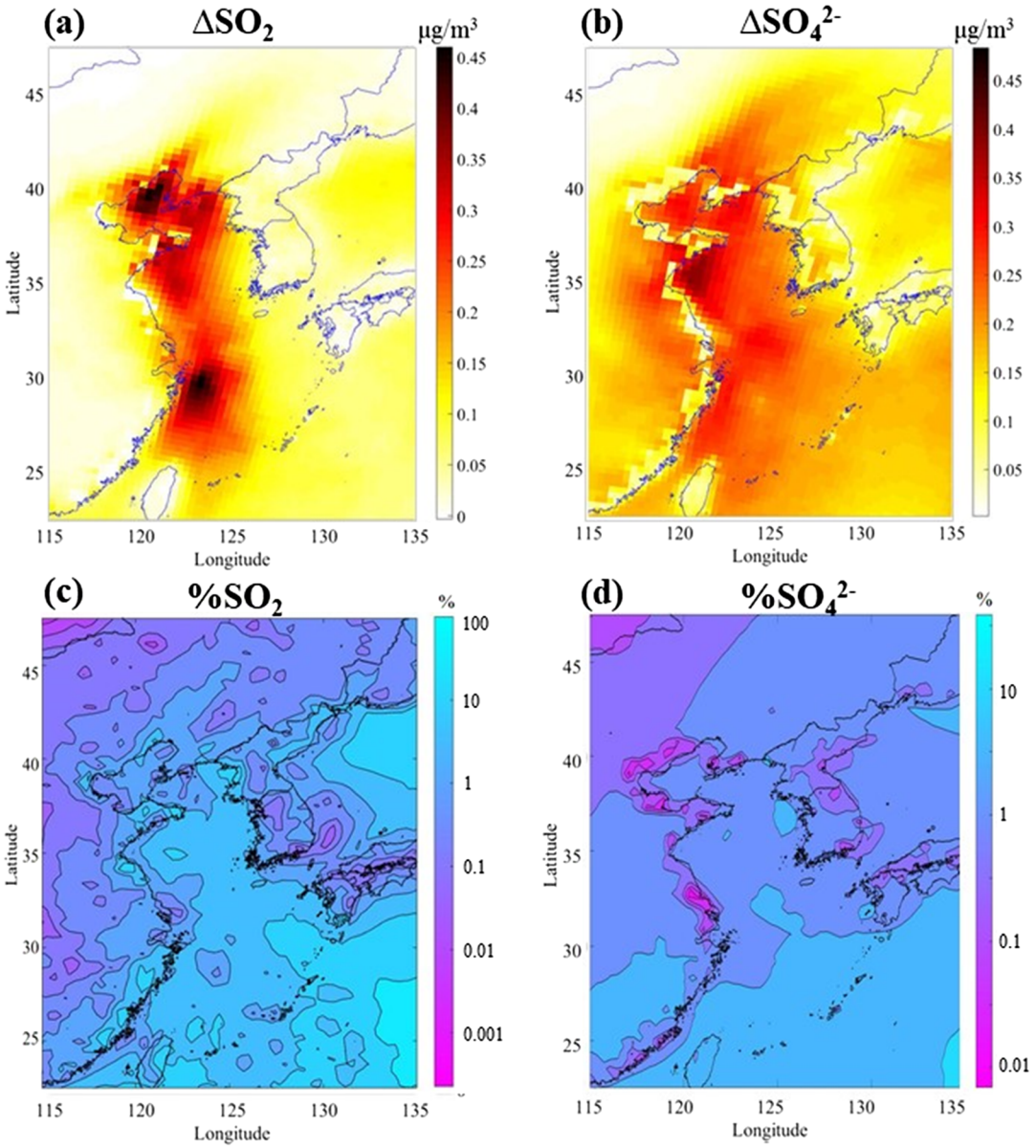


**Figure 6.** Absolute and relative impacts of marine DMS emissions on monthly mean atmospheric (a, c) $SO_2$ and (b, d) $SO_4^{2-}$over Chinese seawater.

### 3.3.1. DMS Contribution to $SO_2$ and $SO_4^{2-}$

The impacts of marine DMS emissions on monthly mean atmospheric $SO_2$ and $SO_4^{2-}$ concentrations are shown in Figure 6. The addition of DMS emissions increases the atmospheric $SO_2$ concentration by 0.1–0.45 μg/m$^3$ primarily over the oceanic areas. Such increases are particularly noticeable in the Bohai Sea and the East China Sea. The high DMS seawater concentrations in the two regions generate elevated DMS emissions, which ultimately lead to increased loading of $SO_2$. The relative contribution of DMS emissions to $SO_2$ is generally less than 10% over the China Seas though the largest impact reaches nearly 20% in coastal areas.

The simulated high atmospheric concentration of $SO_4^{2-}$ in Case C mainly occurs along the coastline of eastern China (Figure S2). The simulated concentrations of $SO_4^{2-}$ over the ocean range between 5 and 15 μg/m$^3$ and are slightly higher than the measured $SO_4^{2-}$ concentrations of 0.9–6.6 μg/m$^3$ in the 2018 Cruise Survey Experiment. The addition of DMS emissions increases the atmospheric concentration of $SO_4^{2-}$ by 0.15–0.4 μg/m$^3$. The highest increases occur in the area south of the Shandong Peninsula to the northern

Jiangsu coast (Figure 6b). Unlike $SO_2$, the increase of $SO_4^{2-}$ concentration by DMS is not limited to the areas with large DMS emission flux in China's coastal waters. Oceanic DMS also increases atmospheric $SO_4^{2-}$ by 0.1–0.3 $\mu g/m^3$ over some land and open waters of eastern China. This occurs due to the shorter atmospheric residence time of $SO_2$ compared to the longer residence time of $SO_4^{2-}$, which is mainly distributed in fine particles (Faloona, 2009), so it can affect a larger geographical range. The combined chemistry of $NO_3$, OH, and halogen oxidants oxidizes DMS into $SO_2$, which subsequently increases $SO_4^{2-}$. The result is an increase in the acidity of the aerosol, which has important atmospheric significance for the formation of secondary aerosols. In general, the marine DMS emissions increase $SO_2$ and $SO_4^{2-}$ over China's waters and some coastal land areas. However, the relative contributions are generally below 10%, which means the influence of anthropogenic sources play a dominant role in summer.

#### 3.3.2. DMS Potential Contribution to the Total Atmospheric Sulfur Burden Through MSA/nss-$SO_4^2$

DMS emitted from the ocean is oxidized into MSA and $SO_4^{2-}$ in the atmosphere. $SO_2$ generated from combustion of fossil fuels is also oxidized into $SO_4^{2-}$, which can reach the offshore sea area through advection of wind. Therefore, nss-$SO_4^{2-}$ (nonsea salt $SO_4^{2-}$) is derived from the two pathways: DMS released by marine organisms and anthropogenically emitted $SO_2$. It is believed that the only source of MSA in the atmosphere is DMS oxidation, and thus, MSA has been proposed as a commonly used tracer to separate $SO_4^{2-}$ of marine biogenic origin from other sources. A high MSA/nss-$SO_4^{2-}$ ratio suggests a relatively large marine biogenic contribution to the total atmospheric sulfur burden. The predicted concentrations (Case C) of MSA remain at relatively low levels (0.056 $\mu g/m^3$ on average) and reach a high value of ~0.1 $\mu g/m^3$ in Bohai Bay. The spatial distribution of MSA concentration in the atmosphere is consistent with that of the atmospheric DMS concentration (Figure S3). These results agree with previous observations, such as those by Song et al. (2016) who measured an average MSA concentration of 0.062 $\mu g/m^3$ in summer in the Bohai Sea and the Yellow Sea. The mean concentration of nss-$SO_4^{2-}$ remains at relatively high levels of 12 $\mu g/m^3$ in coastal waters due to the large impact of anthropogenic pollution. The highest values of nss-$SO_4^{2-}$ exceed 60 $\mu g/m^3$ in the coastal of the Bohai Bay and East China Sea. Previous studies also reported that the maximum atmospheric nss-$SO_4^{2-}$ concentrations exceeded 40 $\mu g/m^3$ at coastal Qingdao in East China Sea (Gao et al., 1996) and 22 $\mu g/m^3$ near the pier in Shanghai, China (Chen et al., 2012). Although the magnitude and distribution of MSA are consistent with previous studies, the background average value of nss-$SO_4^{2-}$ is higher due to the significant impact of anthropogenic activity in coastal areas like high shipping traffic in east China Seas (Fan et al., 2016). Thus, the average ratio of MSA/nss-$SO_4^{2-}$ is relatively low (<2%). Figure S4 presents a time series of the daytime (8:00–20:00) contribution of DMS to nss-$SO_4^{2-}$ over a selected area of the East China Sea with a relatively higher DMS impact. The contribution varies from day to day. However, the contribution reaches a maximum of ~35% and exceeds 30% on several days. Although the average contribution of DMS to nss-$SO_4^{2-}$ is relatively small over the entire simulated sea area, the average daytime contribution of DMS to nss-$SO_4^{2-}$ over this area is 8.0%. Although the contributions of terrestrial pollution emissions to the marine atmosphere are predominant, the DMS emissions in China's waters can also be a moderately important source for nss-$SO_4^{2-}$.

### 3.4. Comparison of Model Results With Observed $SO_2$ and $PM_{2.5}$ in China

The performance of the model with and without the DMS chemistry is evaluated by comparing the model predictions with monthly mean observed $SO_2$ and fine particles ($PM_{2.5}$) at eight coastal cities in China (Figure 7). At some cities (Zhuhai and Xiamen), the model with DMS emissions does not alter $SO_2$ predictions. However, the model with DMS emissions increases $SO_2$ concentrations by small margins (<0.5 $\mu g/m^3$) at Zhoushan, Shanghai, Nantong, Qingdao, Tianjin, and Qinhuangdao compared to those without the DMS emissions. For several cities in east China region (Zhoushan, Shanghai, Nantong, and Qinhuangdao), the model without DMS emissions marginally overestimates (<1.3 $\mu g/m^3$) $SO_2$ concentrations compared to the observed data likely due to the use of emissions estimates for 2016. Under the influence of sulfur emission reduction policies during 2016–2018, $SO_2$ emissions exhibited decreasing trends in East China, while for southern cities (Zhuhai and Xiamen) with low background $SO_2$ emissions no decreasing trend was found (Li & Bai, 2019). The model with DMS emissions marginally (<1.5 $\mu g/m^3$) deteriorates the comparison with observed $SO_2$ concentrations at Zhoushan, Shanghai, Nantong, and Qinhuangdao but marginally (<0.7 $\mu g/m^3$) improves the comparison at Qingdao and Tianjin. Predicted $PM_{2.5}$ concentrations

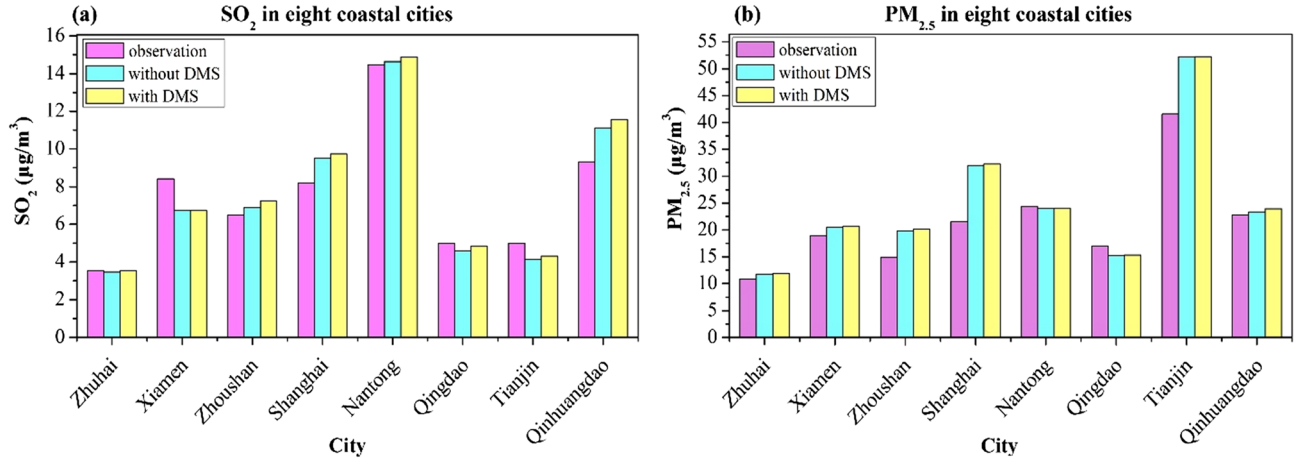


**Figure 7.** A comparison of model predictions (Case A and Case C) with monthly mean observed surface concentrations of a $SO_2$ b $PM_{2.5}$ at eight coastal cities in China in July 2018.

without DMS emissions are generally greater (<10.6 μg/m$^3$) than the observed $PM_{2.5}$ values. The addition of DMS emissions has negligible impact on the $PM_{2.5}$ concentrations at these locations. Model predictions cannot be compared with observed atmospheric $SO_4^{2-}$ concentrations as measured data are not readily available for the study period in China.

## 4. Conclusions

A national scale database of DMS concentration in China seawaters is developed by combining the measured DMS concentrations in China's continental shelf waters with DMS concentrations in seawater from the global database. The database is used to calculate DMS emission fluxes over China's seawater using three different parametrization schemes: LM86, N00, and W92. The impacts of the resulting DMS emissions on the offshore environment of China are examined using the CMAQ model with meteorological fields from WRF and emissions estimates from the joint inventory of terrestrial and shipping emissions.

By comparing the measured DMS concentrations in the Yellow Sea and East China Sea, we find that the use of DMS concentration from the global database significantly underestimates the DMS emissions, while the local database better reproduces DMS emission fluxes over China's seawater. The LM86 parameterization (Liss & Merlivat, 1986) produces the best performance among the three schemes in China's offshore waters. The impacts of marine DMS emissions on regional air quality in the continental shelf of eastern China are examined using the local DMS database and the LM86 parameterization. The model results suggest that the marine DMS emissions increase $SO_2$ and $SO_4^{2-}$ in the atmosphere of the eastern China Sea, with the monthly mean summertime $SO_2$ concentration increasing by 0.1–0.45 μg/m$^3$, and the $SO_4^{2-}$ concentration increasing by 0.15–0.45 μg/m$^3$. The affected areas include not only the offshore areas where DMS emissions are high but also some land areas and distant seas of eastern China. Overall, the contribution of DMS emissions to $SO_2$, $SO_4^{2-}$, and nss-$SO_4^{2-}$ is less than 10%, and anthropogenic sources play a dominate role in this region. The study period covers only a summer month; future studies are needed to investigate the long-term impact of DMS emissions on air quality in China.

## Conflict of Interest

The authors declare no conflicts of financial interest.

## Data Availability Statement

The CMAQ v5.2 and WRF v3.6 model used in this study can be downloaded at https://zenodo.org/record/1167892 and https://www2.mmm.ucar.edu/wrf/users/download/get_source.html, respectively. The Final Analysis (FNL) meteorological data requires authorized access at https://rda.ucar.edu/datasets/ds083.2/

index.html (10.5065/D6M043C6). The MEIC and MIX emission inventory data are available after login at http://meicmodel.org/dataset-meic.html and http://meicmodel.org/dataset-mix.html, respectively. The default global dataset *and the newly developed local data set* of DMS *can be* openly accessed at http://saga.pmel.noaa.gov/dms/ *and* https://dataverse.harvard.edu/dataset.xhtml?persistentId=doi:10.7910/DVN/P4ODKS, respectively. Observations of major pollutants in the air can be freely downloaded from http://data.cma.cn.

**Acknowledgments**
This work was supported by the National Key Research and Development Program of China (Grant 2016YFA060130X), the National Natural Science Foundation of China (Grant 21677038), and the Major Program of Shanghai Committee of Science and Technology, China (19DZ1205009). The views expressed in this paper are those of the authors and do not necessarily represent the views or policies of the U.S. EPA. This manuscript has gone through review process within the Agency and cleared for publication.

## References

Andreae, M. O., & Raemdonck, H. (1983). Dimethyl sulfide in the surface ocean and the marine atmosphere: A global view. *Science*, *221*, 744–747. https://doi.org/10.1126/science.221.4612.744

Atkinson, R., Baulch, D. L., Cox, R. A., Crowley, J. N., Hampson, R. F., Hynes, R. G., et al. (2004). Evaluated kinetic and photochemical data for atmospheric chemistry: Volume I—Gas phase reactions of $O_x$, $HO_x$, $NO_x$ and $SO_x$ species. *Atmospheric Chemistry and Physics*, *4*, 1461–1738. https://doi.org/10.5194/acp-4-1461-2004

Barnes, I., Hjorth, J., & Mihalopoulos, N. (2006). Dimethyl sulfide and dimethyl sulfoxide and their oxidation in the atmosphere. *Chemical Review*, *106*, 940–975. https://doi.org/10.1021/cr020529+

Bates, T. S., Lamb, B. K., Guenther, A., Dignon, J., & Stoiber, R. E. (1992). Sulfur emissions to the atmosphere from natural sourees. *Journal of Atmospheric Chemistry*, *14*, 315–337. https://doi.org/10.1007/BF00115242

Boucher, O., Moulin, C., Belviso, S., Aumont, O., Bopp, L., Cosme, E., et al. (2003). DMS atmospheric concentrations and sulphate aerosol indirect radiative forcing: A sensitivity study to the DMS source representation and oxidation. *Atmospheric Chemistry and Physics*, *3*(1), 49–65. https://doi.org/10.5194/acp-3-49-2003

Breider, T. J., Chipperfield, M. P., Richards, N. A. D., Carslaw, K. S., Mann, G. W., & Spracklen, D. V. (2010). Impact of BrO on dimethylsulfide in the remote marine boundary layer. *Geophysical Research Letters*, *37*, L02807. https://doi.org/10.1029/2009GL040868

Charlson, R. J., Lovelock, J. E., Andreae, M. O., & Warren, S. G. (1987). Oceanic phytoplankton, atmospheric sulfur, cloud albedo and climate. *Nature*, *326*, 655–661. https://doi.org/10.1038/326655a0

Chen, L., Wang, J., Gao, Y., Xu, G., Yang, X., Lin, Q., & Zhang, Y. (2012). Latitudinal distributions of atmospheric MSA and MSA/nss-$SO_4^{2-}$ ratios in summer over the high latitude regions of the Southern and Northern Hemispheres. *Journal of Geophysical Research*, *117*, D10306. https://doi.org/10.1029/2011JD016559

Faloona, I. (2009). Sulfur processing in the marine atmospheric boundary layer: A review and critical assessment of modeling uncertainties. *Atmospheric Environment*, *43*(18), 2841–2854. https://doi.org/10.1016/j.atmosenv.2009.02.043

Fan, Q. Z., Zhang, Y., Ma, W. C., Ma, H., Feng, J. L., Yu, Q., et al. (2016). Spatial and seasonal dynamics of ship emissions over the Yangtze River Delta and East China Sea and their potential environmental influence. *Environmental Science and Technology*, *50*, 1322–1329. https://doi.org/10.1021/acs.est.5b03965

Feng, J. L., Zhang, Y., Li, S. S., Mao, J. B., Patton, A. P., Zhou, Y. Y., et al. (2019). The influence of spatiality on shipping emissions, air quality and potential human exposure in the Yangtze River Delta/Shanghai, China. *Atmospheric Chemistry and Physics*, *19*, 6167–6183. https://doi.org/10.5194/acp-19-6167-2019

Gao, Y., Arimoto, R., Duce, R. A., Chen, L. Q., Zhou, M. Y., & Gu, D. Y. (1996). Atmospheric non-sea-salt sulfate, nitrate, and methanesulfonate over the China Sea. *Journal of Geophysical Research*, *101*, 12,601–12,611. https://doi.org/10.1029/96JD00866

Hoffmann, E. H., Tilgner, A., Schrödner, R., Bräuer, P., Wolke, R., & Herrmann, H. (2016). An advanced modeling study on the impacts and atmospheric implications of multiphase dimethyl sulfide chemistry. *Proceedings of the National Academy of Sciences*, *113*, 11,776–11,781. https://doi.org/10.1073/pnas.1606320113

Hu, M., Tang, X. Y., Li, J. L., & Ma, Q. J (2003). Distributions of dimethylsulfide in the Bohai Sea and Yellow Sea of China. *Journal of Environmental Sciences*, *15*(006), 762–767. https://doi.org/10.3321/j.issn:1001-0742.2003.06.007

Jenny, L., Svensson, G., Wisthaler, A., Tjernström, M., Hansel, A., & Leck, C. (2010). The vertical distribution of atmospheric DMS in the high arctic summer. *Tellus, Series B: Chemical and Physical Meteorology*, *62*, 160–171. https://doi.org/10.1111/j.1600-0889.2010.00458.x

Kettle, A. J., Andreae, M. O., Amouroux, D., Andreae, T. W., Bates, T. S., Berresheim, H., et al. (1999). A global database of sea surface dimethylsulfide (DMS) measurements and a procedure to predict sea surface DMS as a function of latitude, longitude, and month. *Global Biogeochemical Cycles*, *13*, 399–444. https://doi.org/10.1029/1999gb900004

Kondo, J. (1975). Air-sea bulk transfer coefficients in diabatic conditions. *Boundary-Layer Meteorology*, *9*, 91–112. http://doi.org/10.1007/bf00232256

Lana, A., Bell, T. G., Simó, R., Vallina, S. M., Ballabrera-Poy, J., Kettle, A. J., et al. (2011). An updated climatology of surface dimethlysulfide concentrations and emission fluxes in the global ocean. *Global Biogeochemical Cycles*, *25*, GB1004. http://doi.org/10.1029/2010GB003850

Li, C. X., Yang, G. P., Wang, B. D., & Xu, Z. J. (2016). Vernal distribution and turnover of dimethylsulfide (DMS) in the surface water of the Yellow Sea. *Journal of Geophysical Research: Oceans*, *121*, 7495–7516. https://doi.org/10.1002/2016JC011901

Li, J. P., Zhang, H. H., & Yang, G. P. (2015). Distribution of biogenic organic dimethylated sulfur compounds and its influencing factors in the East China Sea in summer. *Environmental Science*, *36*, 49–55. http://doi.org/10.13227/j.hjkx.2015.01.007

Li, K., & Bai, K. (2019). Spatiotemporal associations between $PM_{2.5}$ and $SO_2$ as well as $NO_2$ in China from 2015 to 2018. *International Journal of Environmental Research and Public Health*, *16*(13), 2352. https://doi.org/10.3390/ijerph16132352

Li, M., Zhang, Q., Kurokawa, J. I., Woo, J. H., He, K., Lu, Z., et al. (2017). MIX: A mosaic Asian anthropogenic emission inventory under the international collaboration framework of the MICs-Asia and HTAP. *Atmospheric Chemistry and Physics*, *17*(2), 935–963. http://doi.org/10.5194/acp-17-935-2017

Li, S., Zhang, Y., Zhao, J., Sarwar, G., & Saiz-Lopez, A. (2020). Regional and urban-scale environmental influences of oceanic dms emissions over coastal China seas. *Atmosphere*, *11*, 849. https://doi.org/10.3390/atmos11080849

Liss, P. S., & Merlivat, L. (1986). Air-sea gas exchange rates: Introduction and synthesis. In P. Buat-Menard (Ed.), *The Role of Air-Sea Gas Exchange in Geochemical Cycling* (pp. 113–127). Dordrecht, Netherlands: D. Reidel. https://doi.org/10.1007/978-94-009-4738-2_5

Mahajan, A. S., Fadnavis, S., Thomas, M. A., Pozzoli, L., Gupta, S., Royer, S.-J., et al. (2015). Quantifying the impacts of an updated global dimethyl sulfide climatology on cloud microphysics and aerosol radiative forcing. *Journal of Geophysical Research: Atmospheres*, *120*, 2524–2536. https://doi.org/10.1002/2014JD022687

Marandino, C. A., De Bruyn, W. J., Miller, S. D., & Saltzman, E. S. (2009). Open ocean DMS air/sea fluxes over the eastern South Pacific Ocean. *Atmospheric Chemistry and Physics*, *9*(2), 345–356. https://doi.org/10.5194/acp-9-345-2009

Mathur, R., Xing, J., Gilliam, R., Sarwar, G., Hogrefe, C., Pleim, J., et al. (2017). Extending the Community Multiscale Air Quality (CMAQ) modeling system to hemispheric scales: Overview of process considerations and initial applications. *Atmospheric Chemistry and Physics*, *17*, 12,449–12,474. https://doi.org/10.5194/acp-17-12449-2017

Mcgillis, W. R., Dacey, J. W. H., Frew, N. M., Bock, E. J., & Nelson, R. K. (2000). Water-air flux of dimethylsulfide. *Journal of Geophysical Research*, *105*(C1), 1187–1193. http://doi.org/10.1029/1999JC900243

Muñiz-Unamunzaga, M., Borge, R., Sarwar, G., Gantt, B., de la Paz, D., Cuevas, C. A., & Saiz-Lopez, A. (2018). The influence of ocean halogen and sulfur emissions in the air quality of a coastal megacity: The case of Los Angeles. *Science of Total Environment*, *610-611*, 1536–1545. http://doi.org/10.1016/j.scitotenv.2017.06.098

Nightingale, P. D., Malin, G., Law, C. S., Watson, A. J., Liss, P. S., Liddicoat, M. I., et al. (2000). In situ evaluation of air-sea gas exchange parameterizations using novel conservative and volatile tracers. *Global Biogeochemical Cycles*, *14*(1), 373–387. http://doi.org/10.1029/1999GB900091

Otte, T. L., & Pleim, J. E. (2010). The Meteorology-Chemistry Interface Processor (MCIP) for the CMAQ modeling system: Updates through MCIPv3.4.1. *Geoscientific Model Development*, *3*, 243–256. https://doi.org/10.5194/gmd-3-243-2010

Putaud, J. P., & Nguyen, B. C. (1996). Assessment of dimethylsulfide sea-air exchange rate. *Journal of Geophysical Research*, *101*(D2), 4403–4411. http://doi.org/10.1029/95JD02732

Ravishankara, A. R., Rudich, Y., Talukdar, R., & Barone, S. B. (1997). Oxidation of atmospheric reduced sulphur compounds: Perspective from laboratory studies. *Philosophical Transactions of the Royal Society B: Biological Sciences*, *352*(1350), 171–182. https://doi.org/10.1098/rstb.1997.0012

Saiz-Lopez, A., Plane, J. M. C., Cuevas, C. A., Mahajan, A. S., Lamarque, J. F., & Kinnison, D. E. (2016). Nighttime atmospheric chemistry of iodine. *Atmospheric Chemistry and Physics*, *16*, 15,593–15,604. http://doi.org/10.5194/acp-16-15593-2016

Saltzman, E. S., King, D. B., Holmen, K., & Leck, C. (1993). Experimental determination of the diffusion coefficient of dimethylsulfide in water. *Journal of Geophysical Research*, *98*(C9), 16,481–16,486. https://doi.org/10.1029/93JC01858

Sarwar, G., Gantt, B., Foley, K., Fahey, K., Spero, T. L., Kang, D., et al. (2019). Influence of bromine and iodine chemistry on annual, seasonal, diurnal, and background ozone: CMAQ simulations over the Northern Hemisphere. *Atmospheric Environment*, *213*(395–404), 2019.

Sarwar, G., Gantt, B., Schwede, D., Foley, K., Mathur, R., & Saiz-Lopez, A. (2015). Impact of enhanced ozone deposition and halogen chemistry on tropospheric ozone over the Northern Hemisphere. *Environmental Science and Technology*, *49*, 9203–9211. http://doi.org/10.1021/acs.est.5b01657

Sarwar, G., Xing, J., Fahey, K., Foley, K., Wong, D., Mathur, R., et al. (2018). Dimethylsulfide chemistry: Annual, seasonal, and spatial impacts on sulfate. In *Springer Proceedings in Complexity* (pp. 347–352). Germany, Berlin/Heidelberg: Springer. https://doi.org/10.1007/978-3-319-57645-9_55

Shen, P. P., Tang, Y. N., Liu, H. J., Li, G., Wang, Y., & Qi, Y. Z. (2016). Dimethylsulfide and dimethylsulfoniopropionate production along coastal waters of the northern South China Sea. *Continental Shelf Research*, *117*, 118–125. https://doi.org/10.1016/j.csr.2016.02.003

Skamarock, W. C., & Klemp, J. B. (2008). A time-split nonhydrostatic atmospheric model for weather research and forecasting applications. *Journal of Computational Physics*, *227*(7), 3465–3485.

Song, Y. C., Zhou, S. J., Zhang, H. H., & Yang, G. P. (2016). Distribution and chemical characteristics of water soluble ions in particulate matter over the Yellow Sea and the Bohai Sea in Summer. *Research of Environmental Sciences*, *11*, 1575–1581. https://doi.org/10.13198/j.issn.1001-6929.2016.11.02

Stark, H., Brown, S. S., Goldan, P. D., Aldener, M., Kuster, W. C., Jakoubek, R., et al. (2007). Influence of nitrate radical on the oxidation of dimethyl sulfide in a polluted marine environment. *Journal of Geophysical Research*, *112*, D10S10. https://doi.org/10.1029/2006JD007669

Tesdal, J.-E., Christian, J. R., Monahan, A. H., & von Salzen, K. (2016). Evaluation of diverse approaches for estimating sea-surface DMS concentration and air–sea exchange at global scale. *Environmental Chemistry*, *13*(2), 390–412. https://doi.org/10.1071/en14255

Toumi, R. (1994). BrO as a sink for dimethylsulphide in the marine atmosphere. *Geophysical Research Letters*, *21*, 117–120. https://doi.org/10.1029/93gl03536

Uzuka, N., Watanabe, S., & Tsunogai, S. (1996). Dimethylsulfide in coastal zone of the East China Sea. *Journal of Oceanography*, *52*(3), 313–321. https://doi.org/10.1007/bf02235926

von Glasow, R., & Crutzen, P. J. (2004). Model study of multiphase DMS oxidation with a focus on halogens. *Atmospheric Chemistry and Physics*, *4*, 589–608. https://doi.org/10.5194/acp-4-589-2004

von Glasow, R., Sander, R., Bott, A., & Crutzen, P. J. (2002). Modeling halogen chemistry in the marine boundary layer 1. Cloud-free MBL. *Journal Geophysical Research*, *107*, 4341. https://doi.org/10.1029/2001JD000942

Wanninkhof, R. (1992). Relationship between wind speed and gas exchange over the ocean. *Journal of Geophysical Research*, *97*, 7373–7382. https://doi.org/10.1029/92JC00188

Xu, L., Cameron-Smith, P., Russell, L. M., Ghan, S. J., Liu, Y., Elliott, S., et al. (2016). DMS role in ENSO cycle in the tropics. *Journal of Geophysical Research: Atmospheres*, *121*, 13,537–13,558. https://doi.org/10.1002/2016JD025333

Yang, G. P., Liu, X. T., Li, L., & Zhang, Z. B. (1999). Biogeochemistry of dimethylsulfide in the South China Sea. *Journal of Marine Research*, *57*, 189–211. https://doi.org/10.1357/002224099765038616

Yang, G. P., Song, Y. Z., Zhang, H. H., Li, C. X., & Wu, G. W. (2014). Seasonal variation and biogeochemical cycling of dimethylsulfide (DMS) and dimethylsulfoniopropionate (DMSP) in the Yellow Sea and Bohai Sea. *Journal of Geophysical Research: Oceans*, *119*, 8897–8915. https://doi.org/10.1002/2014JC010373

Yang, G. P., Zhang, H. H., Su, L. P., & Zhou, L. M. (2009). Biogenic emission of dimethylsulfide (DMS) from the North Yellow Sea, China and its contribution to sulfate in aerosol during summer. *Atmospheric Environment*, *43*, 2196–2203. https://doi.org/10.1016/j.atmosenv.2009.01.011

Yang, G. P., Zhang, H. H., Zhou, L. M., & Yang, J. (2011). Temporal and spatial variations of dimethylsulfide (DMS) and dimethylsulfoniopropionate (DMSP) in the East China Sea and the Yellow Sea. *Continental Shelf Research*, *31*, 1325–1335. https://doi.org/10.1016/j.csr.2011.05.001

Yang, G. P., Zhang, S. H., Zhang, H. H., Yang, J., & Liu, C. Y. (2015). Distribution of biogenic sulfur in the Bohai Sea and northern Yellow Sea and its contribution to atmospheric sulfate aerosol in the late fall. *Marine Chemistry*, *169*, 23–32. https://doi.org/10.1016/j.marchem.2014.12.008

Yang, G. P., Zhuang, G. C., Zhang, H. H., Dong, Y., & Yang, J. (2012). Distribution of dimethylsulfide and dimethylsulfoniopropionate in the Yellow Sea and the East China Sea during spring: Spatio-temporal variability and controlling factors. *Marine Chemistry*, *138–139*, 21–31. https://doi.org/10.1016/j.marchem.2012.05.003

Yang, J., Yang, G. P., Zhang, H. H., & Zhang, S. H. (2015). Spatial distribution of dimethylsulfide and dimethylsulfoniopropionate in the Yellow Sea and Bohai Sea during summer. *Chinese Journal of Oceanology and Limnology*, *33*(4), 1020–1038. https://doi.org/10.1007/s00343-015-4188-5

Zhang, S. H., Sun, J., Liu, J. L., Wang, N., Zhang, H. H., Zhang, X. H., & Yang, G. P. (2017). Spatial distributions of dimethyl sulfur compounds, DMSP-lyase activity, and phytoplankton community in the East China Sea during fall. *Biogeochemistry*, *133*, 59–72. https://doi.org/10.1007/s10533-017-0308-y

Zhu, L., Nenes, A., Wine, P. H., & Nicovich, J. M. (2006). Effects of aqueous organosulfur chemistry on particulate methanesulfonate to non-sea salt sulfate ratios in the marine atmosphere. *Journal of Geophysical Research*, *111*, D05316. https://doi.org/10.1029/2005JD006326

## References From the Supporting Information

Atkinson, R., Baulch, D. L., Cox, R. A., Crowley, J. N., Hampson, R. F., Hynes, R. G., et al. (2006). Evaluated kinetic and photochemical data for atmospheric chemistry: Volume II—Gas phase reactions of organic species. *Atmospheric Chemistry and Physics*, *6*, 3625–4055. https://doi.org/10.5194/acp-6-3625-2006

Sander, S. P., Abbatt, J., Barker, J. R., Burkholder, J. B., Friedl, R. R., Golden, D. M., et al. (2016). Chemical kinetics and photochemical data for use in atmospheric studies, Evaluation No. 17. *JPL Publication09–31, 97–4(2000)*, 1135–1151. https://doi.org/10.5167/uzh-52877